

ROBOPIANIST: A Benchmark for High-Dimensional Robot Control

Kevin Zakka^{1,2} Laura Smith¹ Nimrod Gileadi³ Taylor Howell⁴ Xue Bin Peng⁵
Sumeet Singh² Yuval Tassa³ Pete Florence² Andy Zeng² Pieter Abbeel¹
¹UC Berkeley ²Robotics at Google ³DeepMind ⁴Stanford University ⁵Simon Fraser University
<https://kzakka.com/robo pianist/>

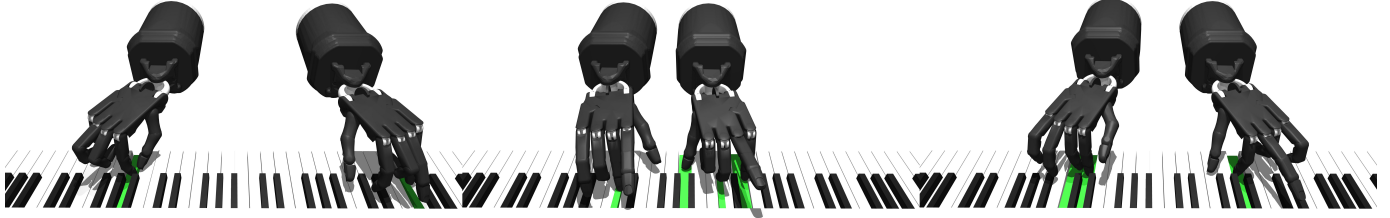


Fig. 1: Policies in the ROBOPIANIST environment displaying skilled piano behaviors such as (1) simultaneously controlling both hands to reach for notes on opposite ends of the keyboard, (2) playing a *chord* with the left hand, which involves precisely and simultaneously hitting a note triplet, and (3) playing a *trill* with the right hand, which involves rapidly alternating between two adjacent notes. To listen to these policies, see <https://kzakka.com/robo pianist/>.

Abstract—We introduce a new benchmarking suite for high-dimensional control, targeted at testing high spatial and temporal precision, coordination, and planning, all with an underactuated system frequently making-and-breaking contacts. The proposed challenge is *mastering the piano* through bi-manual dexterity, using a pair of simulated anthropomorphic robot hands. We call it ROBOPIANIST, and the initial version covers a broad set of 150 variable-difficulty songs. We investigate both model-free and model-based methods on the benchmark, characterizing their performance envelopes. We observe that while certain existing methods, when well-tuned, can achieve impressive levels of performance in certain aspects, there is significant room for improvement. ROBOPIANIST provides a rich quantitative benchmarking environment, with human-interpretable results, high ease of expansion by simply augmenting the repertoire with new songs, and opportunities for further research, including in multi-task learning, zero-shot generalization, multimodal (sound, vision, touch) learning, and imitation. Supplementary information, including videos of our control policies, can be found at <https://kzakka.com/robo pianist/>.

I. INTRODUCTION

As the fields of control and reinforcement learning continue to develop, a key question is how will progress be measured. In fields like computer vision and natural language processing, progress has been fueled by robust, quantifiable, and interpretable benchmarks – which in aggregate achieve *breadth* [1], and in each explore complementary focuses in *depth*: take for example the famous challenge of “Winograd schema” [2], first proposed in 1972 and later developed in 2012 [3] into an influential benchmark. While in control and reinforcement learning, certain benchmarking efforts have begun both to aggregate [4] and explore different aspects of depth, a particularly under-served area has been robust benchmarks which focus on high-dimensional control, including in particular the perhaps ultimate “challenge problem” of high-dimensional robotics:

mastering bi-manual (two-handed) multi-fingered control.

In fact, despite decades-long research into replicating the dexterity of the human hand, high-dimensional control remains a grand challenge in robotics. This topic has inspired considerable research from both a mechanical design [5, 6, 7] and control theoretic point of view [8, 9, 10, 11, 12]. While learning-based approaches [13, 14, 15, 16, 17, 18, 19] have dominated the recent literature, the class of problems typically considered corresponds to a limited definition of dexterity. In particular, most all such tasks are well-specified using a single goal-state or termination condition, limiting the complexity of the solution space and oftentimes yielding unnatural-looking behaviors so long as the desired terminal state is reached.

In this work, we introduce a new benchmark suite for high-dimensional control, ROBOPIANIST, where bi-manual simulated anthropomorphic robot hands are tasked with playing a variety of songs (i.e., correctly pressing sequences of keys on a keyboard) conditioned on sheet music, in the form of a Musical Instrument Digital Interface (MIDI) transcription. The robot hands themselves exhibit high degrees of freedom (22 actuators per hand, for a total of 44), and are partially underactuated, akin to human hands. We specifically chose this domain because playing a song successfully means being able to sequence actions in ways that exemplify many of the properties that we look for in high-dimensional control policies, including (i) spatial and temporal precision (hitting the right notes, at the right time), (ii) coordination (simultaneously achieving multiple different goals, in this case, fingers on each hand hitting different notes, without colliding), and (iii) planning (how a key is pressed should be conditioned on the expectation of how it would enable the policy to reach future notes). Additionally, piano playing also presents an immediately *interpretable* task success signal (i.e., “does it

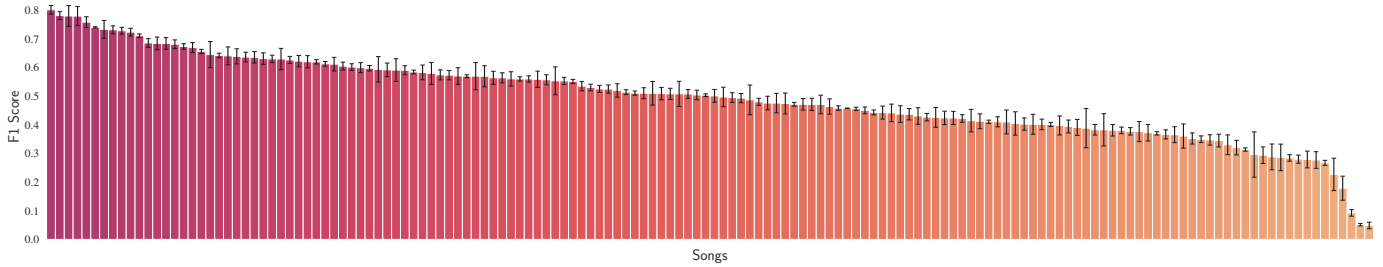


Fig. 2: A full example set of F1 scores on all tasks in ROBOPIANIST-REPertoire-150, highlighting the breadth of difficulty offered by the benchmark. This example set of scores is from the model-free method discussed in Section IV (errors bars represent standard deviations over 3 seeds). Both model-free and model-based implementations as well as evaluations are discussed in Subsection V-B.

sound good?”), and this can e.g., be disentangled from the particular reward/cost functions used.

The initial ROBOPIANIST-Repertoire-150 benchmark covers 150 songs, where each song is effectively a different task. Through extensive experiments, we investigate the performance envelope of both model-free and model-based methods and demonstrate that, while there is ample room for improvement, our policies are able to produce compelling performances. We encourage the reader to watch and listen to the performances at <https://kzakka.com/robopianist/>. For expanding further on the benchmarking suite, since song data is also freely available on the Internet (either by parsing MIDI files, or YouTube data), one can also effectively scale up the number of tasks presented in this domain over time. Figure 2 also shows that we can sort songs (i.e., tasks) by difficulty, reflected in how well a policy can learn the song. Being able to sort tasks via such metrics can foster additional research across a multitude of topics in robot learning, including curriculum learning and transfer learning. Overall, ROBOPIANIST exhibits a straightforward task, easy to simulate environment, clear evaluation metrics, and is amenable to a variety of expansion opportunities in the future. Code for simulation, control and learning, baselines and datasets will be made available at <https://github.com/google-research/robopianist/>.

To summarize, we believe ROBOPIANIST provides many distinct and complementary aspects relative to previous benchmarks for high-dimensional control and is a strong addition to the community for the following reasons:

- **Challenging.** As we show in Subsection V-B, ROBOPIANIST is challenging for model-based and model-free methods. Without a shaped reward in the form of fingering information, they perform poorly, and even with extensive reward shaping, there is plenty room for improvement.
- **Interpretable.** One can simply look at and listen to a policy to gauge its performance.
- **Multimodal.** Playing the piano is sensory-rich: policies can make use of sound, vision and touch.
- **Data rich and extendable.** On top of just adding more MIDI files to expand the number of tasks, one can incorporate other abundant sources of data such as YouTube videos to create third-person demonstrations.
- **Enables knowledge reuse.** Similar songs share note and pattern structures which can be reused to solve new songs zero-shot. More broadly, ROBOPIANIST is a natural playground for studying multi-task and meta-learning.
- **Open source.** We have fully open-sourced the benchmark and dataset at <https://github.com/google-research/robopianist/>.

II. RELATED WORK

We address related work within two primary areas: dexterous high-dimensional control, and robotic pianists.

Dexterous Manipulation and High-Dimensional Control

The vast majority of the control literature uses much lower-dimensional systems (i.e., single-arm, simple end-effectors) than high-dimensional dexterous hands. Specifically, only a handful of general-purpose policy optimization methods have been shown to work on high-dimensional hands, even for a single hand [14, 13, 16, 15, 20, 18, 21, 11], and of these, only a subset has demonstrated results in the real world [14, 13, 16, 15, 20]. Results with bi-manual hands are even rarer, even in simulation only [19, 22].

As a benchmark, perhaps the most distinguishing aspect of ROBOPIANIST is in the definition of “task success”. As an example, general manipulation tasks are commonly framed as the continual application of force/torque on an object for the purpose of a desired change in state (e.g., SE(3) pose and velocity). Gradations of dexterity are predominantly centered around the kinematic redundancy of the arm or the complexity of the end-effector, ranging from parallel jaw-grippers to anthropomorphic hands [23, 19]. A gamut of methods have been developed to accomplish such tasks, ranging from various combinations of model-based and model-free RL, imitation learning, hierarchical control, etc. [24, 14, 17, 16, 25, 26]. However, the class of problems generally tackled corresponds to a definition of dexterity pertaining to traditional manipulation skills [27], such as re-orientation, relocation, manipulating simply-articulated objects (e.g., door opening, ball throwing and catching), and using simple tools (e.g., hammer) [4, 28, 19, 15, 29]. The only other task suite that we know of that presents bi-manual tasks, the recent Bi-Dex [19] suite, presents a broad collection of tasks that fall under this category.

While these works represent an important class of problems, we explore an alternative notion of dexterity and success. In particular, for most all the aforementioned suite of manipulation tasks, the “goal” state is some explicit, specific geometric function of the final states; for instance, an open/closed door, object re-oriented, nail hammered, etc. This effectively reduces the search space for controls to predominantly a single “basin-of-attraction” in behavior space per task. In contrast, the ROBOPIANIST suite of tasks encompasses a more complex notion of a goal, which is encoded through a musical performance. In effect, this becomes a highly combinatorially variable sequence of goal states, extendable to arbitrary difficulty by only varying the musical score. “Success” is graded on accuracy over an entire episode; concretely, via a time-varying non-analytic output of the environment, i.e., the music. Thus, it is not a matter of the “final-state” that needs to satisfy certain termination/goal conditions, a criterion which is generally permissive of less robust execution through the rest of the episode, but rather the behavior of the policy *throughout the episode* needs to be precise and musical.

Similarly, the literature on humanoid locomotion and more broadly, “character control”, another important area of high-dimensional control, primarily features tasks involving the discovery of stable walking/running gaits [30, 31, 32], or the distillation of a finite set of whole-body movement priors [33, 34, 35], to use downstream for training a task-level policy. Task success is typically encoded via rewards for motion progress and/or reaching a terminal goal condition. It is well-documented that the endless pursuit of optimizing for these rewards can yield unrealistic yet “high-reward” behaviors. While works such as [33, 36] attempt to capture *stylistic* objectives via leveraging demonstration data, these reward functions are simply appended to the primary task objective. This scalarization of multiple objectives yields an arbitrarily subjective Pareto curve of optimal policies. In contrast, performing a piece of music entails both objectively measurable precision with regards to melodic and rhythmic accuracy, as well as a subjective measure of musicality. Mathematically, this translates as *stylistic* constraint satisfaction, paving the way for innovative algorithmic advances.

Robotic Piano Playing Robotic pianists have a rich history within the literature, with several works dedicated to the design of specialized hardware [37, 38, 39, 40, 41, 42], and/or customized controllers for playing back a song using pre-programmed commands (open-loop) [43, 44]. The work in [45] leverages a combination of inverse kinematics and trajectory stitching to play single keys and playback simple patterns and a song with a Shadow hand [46]. More recently, in [47], the author simulated robotic piano playing using offline motion planning with inverse kinematics for a 7-DoF robotic arm, along with an Iterative Closest Point-based heuristic for selecting fingering for a four-fingered Allegro hand. Each hand is simulated separately, and the audio results are combined post-hoc. Finally, in [48], the authors formulate piano playing as an RL problem for a single Allegro hand

(four fingers) on a miniature piano, and additionally leverage tactile sensor feedback. However, the tasks considered are rather simplistic (e.g., play up to six successive notes, or three successive chords with only two simultaneous keys pressed for each chord). The ROBOPIANIST benchmark suite is designed to allow a general bi-manual controllable agent to emulate a pianist’s growing proficiency on the instrument by providing a curriculum of musical pieces, graded in difficulty. Leveraging two underactuated anthropomorphic hands as actuators provides a level of realism and exposes the challenge of mastering this suite of high-dimensional control problems.

III. THE ROBOPIANIST BENCHMARK

In this section, we introduce the main elements of the ROBOPIANIST benchmark. We begin by describing the general setup of our benchmark, walk through its practical implementation in simulation, and finally, detail our MIDI dataset which defines the task distribution available in the benchmark.

A. Benchmark setup

States	Unit	Size
Hand joint angles	rad	48
Hand joint velocities	rad/s	48
Forearm positions	m	4
Forearm velocities	m/s	4
Piano key angles	rad	88
Piano key velocities	rad/s	88
Fingering (<i>goal</i>)	discrete	10
Piano key press (<i>goal</i>)	discrete	88
Total		378

Actions	Unit	Size
Desired hand joint angles	rad	40
Desired forearm positions	m	4
Total		44

Observations	Unit	Size
Hand and forearm joints	rad	52
Cartesian forearm position	m	6
Piano key angles	rad	88
Fingering	discrete	10
Piano key press	discrete	88
Previous reward	—	1
Previous action	rad	44
Total		289

TABLE I: The state, action, and observation spaces of the ROBOPIANIST MDP. Fingering is a discrete boolean vector with size equal to the number of fingers, with each component indicating if the corresponding finger is expected to be in contact with a key. This information is extracted from the fingering annotations in the MIDI file for each piece/task.

Learning to play the piano can be formulated as a finite-horizon Markov Decision Process (MDP) defined by a tuple $(\mathcal{S}, \mathcal{A}, \rho, p, r, \gamma, H)$ where $\mathcal{S} \subset \mathbb{R}^n$ is the state space, $\mathcal{A} \subset \mathbb{R}^m$ is the action space, $\rho(\cdot)$ is the initial state distribution, $p(\cdot|s, a)$ governs the dynamics, $r : \mathcal{S} \times \mathcal{A} \rightarrow \mathbb{R}$ defines the rewards, $\gamma \in [0, 1)$ is the discount factor, and H is the horizon. The goal of an agent is to maximize its total expected reward

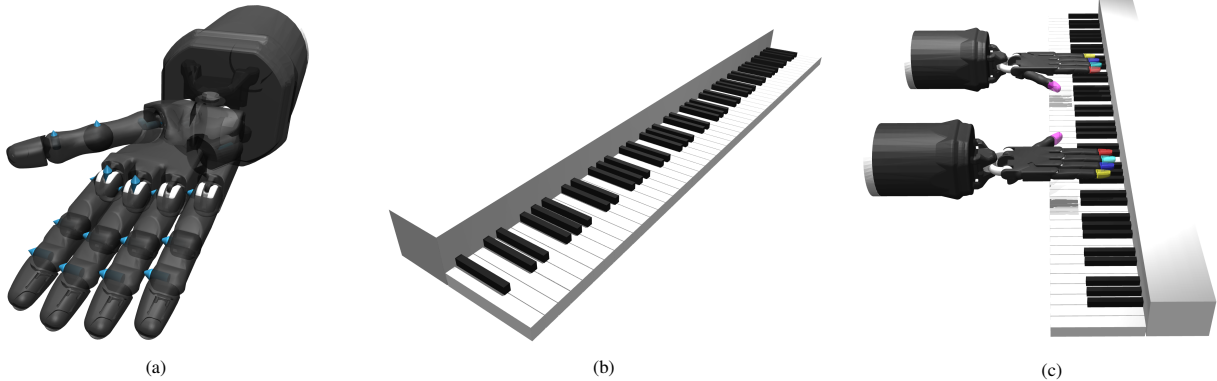


Fig. 3: From left to right, (a): 24 DoF, under-actuated right Shadow Hand model, (b): 88 DoF digital piano model, and (c): ROBOPIANIST task setup with left and right Shadow Hands placed above the piano on an invisible gantry.

over the horizon $\mathbb{E} \left[\sum_{t=0}^H \gamma^t r(s_t, a_t) \right]$. In the ROBOPIANIST benchmark, each song is a separate task with a different note trajectory and horizon H .

All tasks in ROBOPIANIST share the same underlying state, action, and observation spaces (Table I)¹. The action space \mathcal{A} is a 44 dimensional bounded, continuous action corresponding to desired joint positions for the hands and forearms. The desired positions are converted to torques at the 52 joints using proportional-position actuators². In particular, we note that both proprioceptive states (i.e., joint and forearm positions) and exteroceptive states (i.e., key joint positions) are measurements that are readily available in the real world.

A ROBOPIANIST task is illustrated in Figure 3. At episode initialization, the hands are placed in the middle of the keyboard and the MIDI file is converted into a piano roll, i.e., a binary matrix in $\mathbb{Z}^{T \times 88}$, where T is the number of time steps. The piano roll is a time-indexed trajectory telling us which of the 88 notes should be active at every time step, essentially defining a time-varying “goal trajectory.” Each task has a variable length T which is a function of both the MIDI length and the control frequency. At an implementation level, all tasks in ROBOPIANIST are exposed as distinct `dm_env` [49] or `gym` [50] environments, which makes it straightforward to plug them directly into existing RL or imitation learning codebases.

B. Simulation details

We use the open-source MuJoCo [51] simulator with the `dm_control` Python bindings [52]. We chose MuJoCo for a few reasons: 1) faster-than-realtime rigid body simulation in the presence of contacts, 2) MJCF model definition combined with ease of task creation with the `Composer` module, 3) the feature-rich interactive viewer allowing for visual debugging, playback and interaction with the physical models using the

¹The MDP is fully observable, but in practice we use an observation space that is not exactly the state space – for example, to better align with hardware in that there are no direct velocity sensors. Any lack of observability on joint velocities can be remedied simply by incorporating the last two measurements for the agent.

²The control signal for the distal actuator of each non-thumb finger ($4 \cdot 2 = 8$) is split amongst the middle and distal joints.

mouse input, 4) recently, the addition of a high-quality robot models [53] maintained by the creators of the simulator.

Piano model. We create a full-size standard (“88-key”) digital piano in simulation, which consists of 52 white keys and 36 black keys, spanning 12 major scales. We use a Kawai reference manual [54] to closely match the dimensions, shape, positioning and spacing of the keys on the keyboard. Each key is modeled using a linear spring. To speed up the simulation, we explicitly disable collision checking between the white keys since they can’t possibly ever be in contact. Additionally, rather than creating a custom key mesh for the white keys (i.e., a box with a crevice in which the black key rests), we disable collision checking between white and black keys. The result is practically equivalent but faster to simulate since we exclusively deal with primitive box geometries.

Hand model. We use the left and right Shadow Dexterous Hand [46] models from MuJoCo Menagerie [53]. This anthropomorphic hand has been designed to closely reproduce the kinematics and dexterity of the human hand. The Shadow Hand is underactuated: it has 24 degrees of freedom, but only 20 actuators. This is because the non-thumb finger distal joints are coupled. We add two degrees of freedom to the base of the hand forearms to simulate the equivalent of a planar gantry: a prismatic joint to translate laterally along the piano length, and a prismatic joint to translate longitudinally along the piano depth. Note that the Shadow Hand itself provides two rotational degrees of freedom in each wrist (similar to human wrist joint). Since [19] used two copies of a right hand, ROBOPIANIST is the first benchmarking suite we know of that uses both left and right hands, and also does so in a way in which the handedness is relevant (piano pieces are designed for a pair of left and right human hands).

Sound representation. We use the Musical Instrument Digital Interface (MIDI) standard to represent piano pieces and synthesize sounds. Very briefly, a MIDI file stores `note_on` and `note_off` messages. Each such message stores a note number, a note velocity and a timestamp. The MIDI number is an integer between 0 and 127 and encodes a note’s pitch. The velocity is also an integer from 0 to 127 and controls the intensity of the sound. The timestamp specifies when to execute the message. The moment a key is pressed on a piano,

Reward	Formula	Weight	Explanation
Key Press	$0.5 \cdot g(\ k_s - k_g\ _2) + 0.5 \cdot (1 - \mathbf{1}_{\{\text{false positive}\}})$	1	Press the right keys and only the right keys
Forearm Penalty	$1 - \mathbf{1}_{\{\text{collision}\}}$	0.4	Minimize forearm collisions
Energy Penalty	$ \tau_{\text{joints}} ^T v_{\text{joints}} $	-5e-3	Minimize energy expenditure
Finger Close to Key	$g(\ p_f - p_k\ _2)$	1	Shaped reward to bring fingers to key

TABLE II: The reward structure used for the model-free baseline. τ represents the joint torque, v is the joint velocity, p_f and p_k represent the position of the finger and key in the world frame respectively, k_s and k_g represent the current and the goal states of the key respectively, and g is a function that transforms the distances to rewards in the $[0, 1]$ range. See the appendix for a detailed description of each term.

it generates a `note_on` event, and the moment it is released, it generates a `note_off` event. The intensity of the generated sound is controlled by the velocity of the keystroke. In our simulation, a key is considered *active* when its joint position exceeds the halfway point of its range. When this occurs, we emit the `note_on` message. We currently do not model the intensity of each keynote, captured by the velocity dimension in the MIDI representation.

C. MIDI dataset

A contribution of ROBOPIANIST is providing a rich initial song corpora with which we can evaluate high-dimensional control policies. To do this, we identify a dataset developed for research into estimating human fingering for piano, called the PIG dataset [55], and transform it into a corpus of MIDI files that can be played in our simulated environment. This dataset contains piano pieces from twenty-four Western composers spanning the baroque, classical and romantic periods. The pieces vary in difficulty, ranging from relatively easy (e.g., Mozart’s Piano Sonata K 545 in C major) to significantly harder (e.g., Scriabin’s Piano Sonata No. 5). We refer the reader to [55] for a detailed list of the pieces.

The fingering labels are encoded as a 10-dimensional boolean vector, with each component indicating if the corresponding finger is expected to be in contact with a key at that timestep. Note that fingering information is generally quite sparse for most pieces of music, and is usually reserved for particularly tricky sections of the piece. Pianists are expected to rely on their skill and experience with the instrument to discover the most efficient fingering. Further, most fingering markings on sheet music are a general guide, and it is up to the pianist to gracefully incorporate this assistive information and ensure a smooth musical flow. All these factors provide enticing opportunities for the design of a controller’s combinatorial reasoning. In our presented solution methodologies, we incorporate the boolean fingering information within the reward formulation (Table II). For future research enabled by the benchmark, having a policy discover the fingering would be an impressive additional challenge.

D. Evaluation criteria

Agents in ROBOPIANIST are evaluated based on precision, recall and F1 scores. These metrics are computed by comparing the state of the piano keys at every time step with the corresponding ground-truth state stored in the MIDI file, averaged across all time steps. Intuitively, precision measures how good a policy is at not hitting the wrong keys (i.e., low

false positive rate) and recall measures how good it is at hitting the right keys (i.e., low false negative). Thus, a policy that hovers above the keyboard without hitting any keys has high precision but low recall, and conversely, a policy that hits all the keys simultaneously (assuming it were physically possible) has high recall but low precision.

IV. HIGH-DIMENSIONAL ROBOT CONTROL

High-dimensional robot control requires amongst other things, precision in space and time, coordination, planning, and contact. The ROBOPIANIST task suite and dataset stresses precisely these properties in a piano playing environment (Section III). In this section, we describe initial steps towards tackling the benchmark by introducing two popular policy optimization methods, as well as various design considerations we incorporated to improve their performance. These may serve as both (i) expert data generators (e.g., for imitation learning), or (ii) baselines for future work on the benchmark.

A. Baseline methods

There are a variety of method-agnostic criteria and solution regimes that one may be interested in applying to the benchmark. For one, does the policy method itself have access to the true dynamics of the environment (model-based), or must it only learn through trial-and-error interactions with the environment (model-free)? If it needs environment interactions, how many are allowed? Additionally, although the exact cutoff limit of what may be considered “real-time” is dependent on specific compute hardware, the ability of a method to be approximately-fast-enough on common compute hardware in order to synthesize behaviors in real-time, whether through a “direct” feedback policy or through online model predictive control (MPC), is another primary consideration that impacts the eventual deployable regimes on real-world hardware.

As baseline methods, we present both model-free and model-based variants. By their nature, the comparison is somewhat inherently “apples vs. oranges”. For one, the model-based method uses the ground truth dynamics which are not used by the model-free variant. Meanwhile, the model-free variant requires a large number (order of 1 million) environment interactions, whereas the model-based variant requires none. Additionally, the way in which computational resources are consumed differs greatly. As is common for model-free RL, considerable compute is used at training time, but the learned policy is encoded into a learned neural network which runs quickly at inference time (we present results with sub-millisecond feed-forward time on an M1 Max CPU).

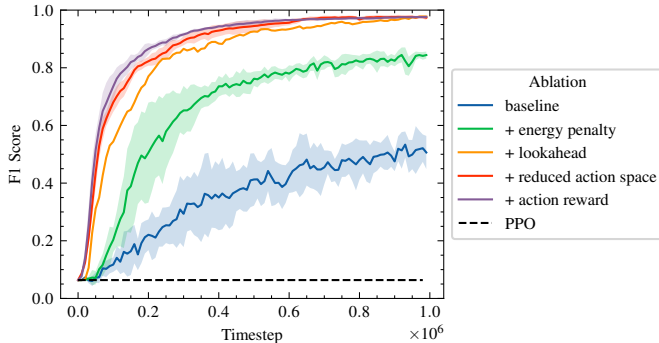


Fig. 4: **ROBOPIANIST-prelude**: Performance of model-free RL with different MDP design considerations. From top to bottom, in the order specified by the legend, each curve **inherits all MDP attributes of the curve before it**, but makes one additional modification as specified by its label. The PPO run, which also inherits all the MDP tweaks, starts making progress at 10M environment interactions, see the appendix for more information.

Meanwhile for model-based MPC with a ground-truth model, it is common for no “training” compute to be required, but instead inference may be computationally intensive, and better results can be obtained simply by expending more inference-time compute. Due to this “apples vs. oranges” nature, our goal is not to proclaim which is “better”, but rather to characterize the performance envelopes of both methods. We choose both to be in the regime of near-real-time policy inference, where we allow the model-based method to slow down simulation time as much as 10% real-time. Model-based methods with additional offline pre-computation are left for future work.

Model-free. The first baseline approach we consider is in the category of model-free reinforcement learning. We present results with the off-policy algorithm DroQ [56], one of several regularized variants of the widely-used Soft-Actor-Critic [57] algorithm, as it is state-of-the-art in terms of performance and sample efficiency. We train a separate policy per-song (multi-task is left for future work) for one million environment interactions using the reward structure in Table II. We found that even with $10\times$ the number of samples, PPO [58] with default Stable Baselines3 [59] hyperparameters was not able to achieve reasonable performance.

Model-based. The second baseline we present uses MPC, and specifically uses the implementation from [60] which was shown to solve the previously-considered-challenging [13, 17, 15] dexterous task of one-handed cube re-orientation in simulation. Specifically amongst the various implementation options presented in [60], we found the most success with the *derivative-free* sampling-based method (“Predictive Sampling”). The cost formulation for the MPC baseline is detailed in the appendix.

Note that while the method with which we received the best success was the derivative-free “Predictive Sampling”, we also tried the optimized *derivative-based* implementation of iLQG [61] also provided by [60], but this was not able to make substantial progress even at significantly slower than real-time speeds. We expect that it should be possible to acquire strong results with derivative-based methods especially with

sufficient reward shaping, both in the near-real-time regime and also with offline model-based trajectory optimization. We note, however, that the (i) high dimensionality, (ii) complex sequence of goals adding many constraints, and (iii) overall temporal length (tens of seconds) of the trajectories pose challenges for some methods that are typically applied to significantly smaller problems.

B. System design

We found that simple modifications to the MDP had a large impact on policy performance. We detail these design considerations and analyze their effect in the following sections.

- **Fingering reward:** We use the fingering annotations from the MIDI dataset to encourage the fingers of the hand to reach the corresponding keys.
- **Lookahead horizon:** Instead of just goal-conditioning the policy for the current timestep, we additionally include the “goal-trajectory” up to some lookahead horizon H into the future.
- **Energy penalty:** We add an extra reward term that penalizes the energy output of the hand actuators, see Table II.
- **Action space reduction:** We reduced the dimensionality of the action space by disabling some DoFs in the hand. We also restricted the range of some actuators.
- **Action-reward:** We appended the action and reward obtained at the previous timestep to the state, see Table II.

V. EXPERIMENTS

The goal of our experiments is twofold. First, to characterize the performance envelope of the algorithms in Section IV and gain insight into the key challenges of the ROBOPIANIST benchmark. Second, to investigate how the MDP structure influences overall policy performance. We study these questions in the context of three experimental setups: ROBOPIANIST-prelude, ROBOPIANIST-etude-12 and ROBOPIANIST-repertoire-150.

A. Experimental setup

ROBOPIANIST-prelude consists of one piece with which one can extensively compare the effects of the design decisions introduced in Subsection IV-B on the model-free RL baseline. For these experiments, we use a 10-second snippet of Mozart’s Twelve Variations on “Ah Vous Dirai-Je, Maman” (a.k.a. Twinkle Twinkle Little Star) – a piece that (i) strikes a good balance in difficulty: it is not too simple (e.g., requires both hands, there exists an ornament, etc.) and not too hard (e.g., there are no chords), and (ii) is universally recognizable and, thus, intuitive for humans to quickly listen to and evaluate qualitative success.

ROBOPIANIST-repertoire-150 considers a dataset of 150 MIDI files and evaluates both algorithms mentioned in Section IV (including the best performing variant of the model-free baseline from **ROBOPIANIST-prelude**).

ROBOPIANIST-etude-12 considers 12 randomly sampled songs from the full repertoire of 150 MIDI files and again,

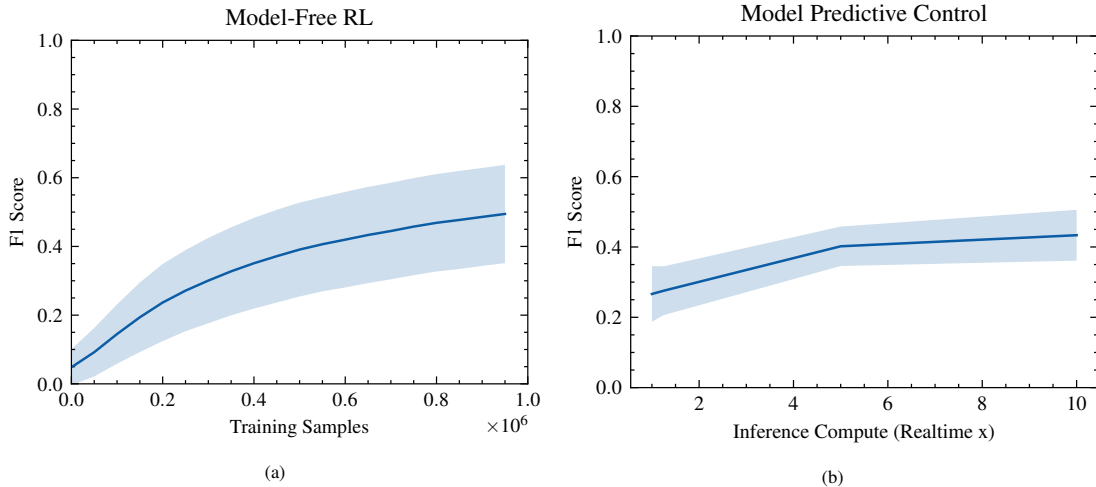


Fig. 6: **ROBOPIANIST-repertoire-150**: (a) Performance of the model-free RL baseline evaluated at checkpoints trained on increasing amounts of environment interactions. Each point corresponds to an average over 150 MIDI files, 3 seeds each, with a standard deviation shading computed over all MIDI files. (b) Performance of the MPC baseline evaluated with an increasing compute budget (e.g., 2 = double the compute used by the same method running realtime). Each point corresponds to an average over 150 songs, with a standard deviation shading computed over all MIDI files.

Heuristic	Pearson Correlation
Notes Per Second	-0.266
Pitch Class Entropy	-0.312
Total Time	-0.383
Max Polyphony	-0.458
Mean Polyphony	-0.447
Unique Pitches	-0.560
Unique Pitch Classes	-0.238
Pitch Range	-0.486

TABLE III: Correlation of musical properties of the MIDI dataset with the performance of the model-free RL baseline as measured by its F1 score on **ROBOPIANIST-repertoire-150**. This shows that for example, *more unique pitches* (different keys pressed) in a song is especially correlated with it being *harder*.

evaluates both of the algorithms mentioned in Section IV. *This etude serves as a proxy for the full repertoire, for smaller scale experiments and/or more modest compute budgets.* For results and analysis on this etude, we refer the reader to the appendix. **Training details.** Training the model-free RL baseline takes approximately 5 hours per song on an Intel Xeon E5-2696V3 Processor hardware with 32 cores (2.3 GHz base clock), 416 GB RAM and 4 Tesla K80 GPUs (n1-highmem-64 machine type on Google Cloud). Inference for both model-free and model-based variants is done on an M1 Max, 64GB RAM processor. All model-free policies are trained and evaluated three times on each task with different random seeds. Model-based policies are evaluated once per task. We implement our model-free baseline using JAX [62], and our MPC baseline using MJPC [60]. Complete hyperparameters and experimental details are listed in the appendix.

B. Overall evaluation

The performance of the model-free RL baseline as well as the MPC baseline on **ROBOPIANIST-repertoire-150** on all 150 tasks is illustrated in Figure 6. See Figure 2 for individual results on all songs for model-free, and the appendix for full results for model-based.

What makes a task hard? We can sort the songs in descending order based on the F1 scores of the model-free RL policies, which presents a birds-eye view of the difficulty between songs (i.e., lower is harder). By measuring the Pearson correlation between the F1 scores against heuristics calculated per song from the 150 MIDI files (shown in Table III), we can observe which task attributes contribute the most to the difficulty.

Interestingly, we observe that the strongest negatively correlated variable is the number of unique pitches (i.e., different keys on the keyboard) – the more there are, the harder the task. This could suggest that the number of unique notes to hit for a task contributes to the diversity of control trajectories that need to be addressed by the policy. This attribute is followed by the second-most negatively correlated variable maximum polyphony, i.e., the average maximum number of notes active at any point in time. Successfully playing multiple notes imposes additional constraints on precision. For high-dimensional control, this could be akin to threading the needle through a more narrow solution space, which can be more challenging to discover with RL through trial and error. These correlations allow us to project difficulty onto new prospective tasks as the dataset expands, and point to interesting areas for future research.

C. Results and baseline studies

The following subsection discusses observations from varying the design decisions detailed in Section IV of the model-free baseline policy on **ROBOPIANIST-prelude**. These observations may continue to be prevalent for related future work in high-dimensional control.

Energy penalty leads to more spatially precise control. High-dimensional control policies trained with RL and random exploration are subject to learning more ecstatic policies (visible with non-smooth trajectories). In particular, these movements deteriorate performance on a task like piano playing, which requires both spatial precision and timing. As

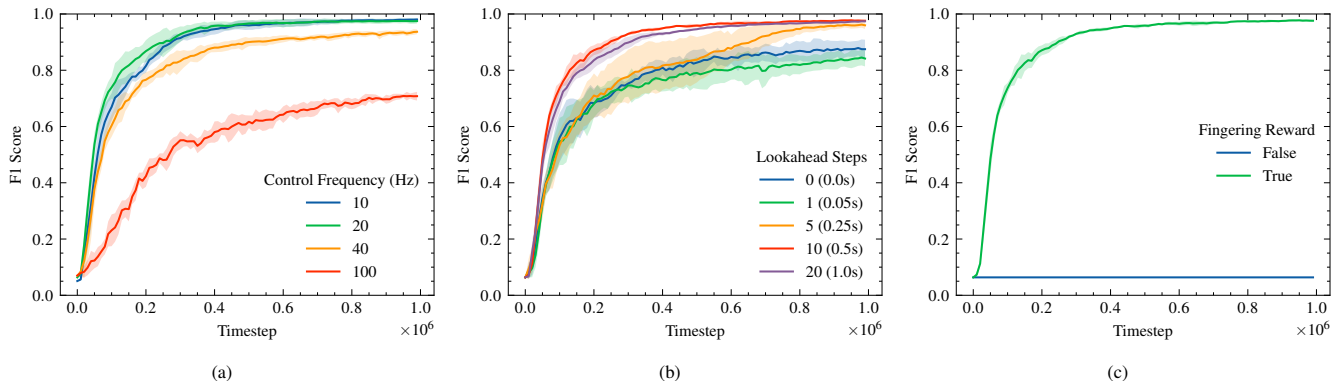


Fig. 7: **ROBOPIANIST-prelude**: (a) Performance of the model-free RL baseline trained with different control frequencies, (b) Performance of the model-free RL baseline trained with different values of the goal lookahead horizon, and (c) Performance of the model-free RL baseline trained with and without a fingering reward.

shown in Figure 4, we observe substantial improvements in quantitative performance (and much less variance) by adding an energy penalty to the policy, which reduces the ecstatic movements and bang-bang-like control during the initial stages of training.

Looking into the future leads to more temporally precise control. We observe additional improvements, both in performance and variance, from appending future goal states (up to a certain horizon) to the goal vector. Intuitively, this allows the policy to plan better for future notes – for example by placing the non-finger joints (e.g., the wrist) in a manner that allows more timely reaching of notes at the next timestep. However, as we show in Figure 7b, increasing the goal lookahead horizon above 0.5 seconds leads to reduced performance.

Reducing the action space trains faster and reduces un-human-like thumb movement. To alleviate exploration even further, we explore the effect of disabling degrees of freedom in the Shadow Hand that either do not exist in the human hand (e.g., the little finger being opposable) or are not strictly necessary for most songs. We additionally reduce the joint range of the thumb, which on the Shadow Hand, can reach backward in a manner not possible on a human hand. As shown in Figure 4, this change leads to faster training. Qualitatively, the change is even more pronounced with the policies trained with the reduced action space exhibiting more natural-looking thumb behaviors (see the project website for a side-by-side comparison).

Fingering information alleviates exploration. Without the fingering reward, the policy struggles to learn meaningful behaviors as shown in Figure 7c.

The control frequency matters. As shown in Figure 7a, the control frequency has a substantial effect on learning. We find that 20Hz is a sweet spot, with notably 100Hz drastically reducing the final score, and 10Hz converging a bit slower. At 100Hz, the MDP becomes too long-horizon, which complicates exploration, and at 10Hz, the discretization of the MIDI file becomes too coarse, which negatively impacts the timing of the notes.

Adding the action and reward to the state helps. As shown in Figure 4, adding the action and reward from the previous

timestep, while marginal, also helps improve the convergence speed of the policy. The previous action helps the policy reason about velocities, which can enable more spatially and temporally precise control. Note we could have obtained a similar effect by stacking a history of past observations – we chose the option that has the smallest increase on its dimension.

VI. DISCUSSION AND CONCLUSION

In this paper, we introduced the ROBOPIANIST benchmark, which provides a simulation framework and suite of tasks in the form of a corpora of songs, together with baseline methods and evaluations, for studying the challenging high-dimensional control problem of mastering piano-playing with bi-manual hands. We showed that both well-tuned model-free and model-based baselines struggle on this benchmark and explored different ways in which to improve them. There is an array of exciting future directions to explore with ROBOPIANIST, including for example: pushing both model-based and model-free methods, using human priors to accelerate learning, studying zero shot generalization to new songs, and using multimodal data like sound and touch.

VII. ACKNOWLEDGMENTS

This project was supported in part by ONR #N00014-22-1-2121 under the Science of Autonomy program.

REFERENCES

- [1] A. Srivastava, A. Rastogi, A. Rao, A. A. M. Shoeb, A. Abid, A. Fisch, A. R. Brown, A. Santoro, A. Gupta, A. Garriga-Alonso, *et al.*, “Beyond the imitation game: Quantifying and extrapolating the capabilities of language models,” *arXiv preprint arXiv:2206.04615*, 2022. 1
- [2] T. Winograd, “Understanding natural language,” *Cognitive psychology*, vol. 3, no. 1, pp. 1–191, 1972. 1
- [3] H. Levesque, E. Davis, and L. Morgenstern, “The winograd schema challenge,” in *Thirteenth international conference on the principles of knowledge representation and reasoning*, 2012. 1

- [4] J. Fu, A. Kumar, O. Nachum, G. Tucker, and S. Levine, “D4RL: Datasets for deep data-driven reinforcement learning,” *arXiv preprint arXiv:2004.07219*, 2020. 1, 2
- [5] S. Yuan, L. Shao, C. L. Yako, A. M. Gruebele, and J. K. Salisbury, “Design and control of roller grasper v2 for in-hand manipulation,” *2020 IEEE/RSJ International Conference on Intelligent Robots and Systems (IROS)*, pp. 9151–9158, 2020. 1
- [6] Z. Xu and E. Todorov, “Design of a highly biomimetic anthropomorphic robotic hand towards artificial limb regeneration,” in *2016 IEEE International Conference on Robotics and Automation (ICRA)*, pp. 3485–3492, 2016. 1
- [7] C. McCann, V. Patel, and A. Dollar, “The stewart hand: A highly dexterous, six-degrees-of-freedom manipulator based on the stewart-gough platform,” *icra*, vol. 28, no. 2, pp. 23–36, 2021. 1
- [8] R. Fearing, “Implementing a force strategy for object re-orientation,” in *Proceedings. 1986 IEEE International Conference on Robotics and Automation*, vol. 3, pp. 96–102, 1986. 1
- [9] D. Rus, “In-hand dexterous manipulation of piecewise-smooth 3-d objects,” *The International Journal of Robotics Research*, vol. 18, no. 4, pp. 355–381, 1999. 1
- [10] A. Okamura, N. Smaby, and M. Cutkosky, “An overview of dexterous manipulation,” in *Proceedings 2000 ICRA. Millennium Conference. IEEE International Conference on Robotics and Automation. Symposia Proceedings (Cat. No.00CH37065)*, vol. 1, pp. 255–262 vol.1, 2000. 1
- [11] T. Pang, H. J. T. Suh, L. Yang, and R. Tedrake, “Global planning for contact-rich manipulation via local smoothing of quasi-dynamic contact models,” *ArXiv*, vol. abs/2206.10787, 2022. 1, 2
- [12] R. R. Ma and A. M. Dollar, “On dexterity and dexterous manipulation,” in *2011 15th International Conference on Advanced Robotics (ICAR)*, pp. 1–7, 2011. 1
- [13] M. Andrychowicz, B. Baker, M. Chociej, R. Józefowicz, B. McGrew, J. W. Pachocki, A. Petron, M. Plappert, G. Powell, A. Ray, J. Schneider, S. Sidor, J. Tobin, P. Welinder, L. Weng, and W. Zaremba, “Learning dexterous in-hand manipulation,” *The International Journal of Robotics Research*, vol. 39, pp. 20 – 3, 2018. 1, 2, 6
- [14] OpenAI, I. Akkaya, M. Andrychowicz, M. Chociej, M. Litwin, B. McGrew, A. Petron, A. Paino, M. Plappert, G. Powell, R. Ribas, J. Schneider, N. A. Tezak, J. Tworek, P. Welinder, L. Weng, Q. Yuan, W. Zaremba, and L. M. Zhang, “Solving rubik’s cube with a robot hand,” *ArXiv*, vol. abs/1910.07113, 2019. 1, 2
- [15] A. Handa, A. Allshire, V. Makoviychuk, A. Petrenko, R. Singh, J. Liu, D. Makoviichuk, K. Van Wyk, A. Zhurkevich, B. Sundaralingam, *et al.*, “Dextreme: Transfer of agile in-hand manipulation from simulation to reality,” *arXiv preprint arXiv:2210.13702*, 2022. 1, 2, 6
- [16] T. Chen, J. Xu, and P. Agrawal, “A system for general in-hand object re-orientation,” in *Conference on Robot Learning*, pp. 297–307, 2022. 1, 2
- [17] A. Nagabandi, K. Konolige, S. Levine, and V. Kumar, “Deep dynamics models for learning dexterous manipulation,” *Conference on Robot Learning (CoRL)*, vol. abs/1909.11652, 2019. 1, 2, 6
- [18] T. Chen, M. Tippur, S. Wu, V. Kumar, E. H. Adelson, and P. Agrawal, “Visual dexterity: In-hand dexterous manipulation from depth,” *ArXiv*, vol. abs/2211.11744, 2022. 1, 2
- [19] Y. Chen, Y. Yang, T. Wu, S. Wang, X. Feng, J. Jiang, S. M. McAleer, H. Dong, Z. Lu, and S.-C. Zhu, “Towards human-level bimanual dexterous manipulation with reinforcement learning,” *arXiv preprint arXiv:2206.08686*, 2022. 1, 2, 4
- [20] H. Qi, A. Kumar, R. Calandra, Y. Ma, and J. Malik, “In-Hand Object Rotation via Rapid Motor Adaptation,” in *Conference on Robot Learning (CoRL)*, 2022. 2
- [21] I. Mordatch, E. Todorov, and Z. Popović, “Discovery of complex behaviors through contact-invariant optimization,” *ACM Trans. Graph.*, vol. 31, jul 2012. 2
- [22] A. M. Castro, F. N. Permenter, and X. Han, “An unconstrained convex formulation of compliant contact,” *IEEE Transactions on Robotics*, 2022. 2
- [23] A. M. Okamura, N. Smaby, and M. R. Cutkosky, “An overview of dexterous manipulation,” in *Proceedings 2000 ICRA. Millennium Conference. IEEE International Conference on Robotics and Automation. Symposia Proceedings (Cat. No. 00CH37065)*, vol. 1, pp. 255–262, IEEE, 2000. 2
- [24] A. Rajeswaran, V. Kumar, A. Gupta, J. Schulman, E. Todorov, and S. Levine, “Learning complex dexterous manipulation with deep reinforcement learning and demonstrations,” *ArXiv*, vol. abs/1709.10087, 2017. 2
- [25] B. Sundaralingam and T. Hermans, “Relaxed-rigidity constraints: kinematic trajectory optimization and collision avoidance for in-grasp manipulation,” *Autonomous Robots*, vol. 43, pp. 469–483, 2019. 2
- [26] I. Radosavovic, X. Wang, L. Pinto, and J. Malik, “State-only imitation learning for dexterous manipulation,” in *2021 IEEE/RSJ International Conference on Intelligent Robots and Systems (IROS)*, pp. 7865–7871, IEEE, 2021. 2
- [27] R. R. Ma and A. M. Dollar, “On dexterity and dexterous manipulation,” in *2011 15th International Conference on Advanced Robotics (ICAR)*, pp. 1–7, IEEE, 2011. 2
- [28] C. Smith, Y. Karayiannidis, L. Nalpantidis, X. Gratal, P. Qi, D. V. Dimarogonas, and D. Kragic, “Dual arm manipulation—a survey,” *Robotics and Autonomous systems*, vol. 60, no. 10, pp. 1340–1353, 2012. 2
- [29] H. J. Charlesworth and G. Montana, “Solving challenging dexterous manipulation tasks with trajectory optimisation and reinforcement learning,” in *International Conference on Machine Learning*, pp. 1496–1506, PMLR, 2021. 2

- [30] N. Heess, D. TB, S. Sriram, J. Lemmon, J. Merel, G. Wayne, Y. Tassa, T. Erez, Z. Wang, S. Eslami, *et al.*, “Emergence of locomotion behaviours in rich environments,” *arXiv preprint arXiv:1707.02286*, 2017. 3
- [31] A. Sharma, S. Gu, S. Levine, V. Kumar, and K. Hausman, “Dynamics-aware unsupervised discovery of skills,” in *International Conference on Learning Representations*, 2020. 3
- [32] S. Tunyasuvunakool, A. Muldal, Y. Doron, S. Liu, S. Bohez, J. Merel, T. Erez, T. Lillicrap, N. Heess, and Y. Tassa, “dm_control: Software and tasks for continuous control,” *Software Impacts*, vol. 6, p. 100022, 2020. 3, 12
- [33] X. B. Peng, Z. Ma, P. Abbeel, S. Levine, and A. Kanazawa, “AMP: Adversarial motion priors for stylized physics-based character control,” *ACM Transactions on Graphics (TOG)*, vol. 40, no. 4, pp. 1–20, 2021. 3
- [34] J. Merel, L. Hasenclever, A. Galashov, A. Ahuja, V. Pham, G. Wayne, Y. W. Teh, and N. Heess, “Neural probabilistic motor primitives for humanoid control,” in *International Conference on Learning Representations*, 2019. 3
- [35] J. Merel, S. Tunyasuvunakool, A. Ahuja, Y. Tassa, L. Hasenclever, V. Pham, T. Erez, G. Wayne, and N. Heess, “Catch & carry: reusable neural controllers for vision-guided whole-body tasks,” *ACM Transactions on Graphics (TOG)*, vol. 39, no. 4, pp. 39–1, 2020. 3
- [36] A. Escontrela, X. B. Peng, W. Yu, T. Zhang, A. Iscen, K. Goldberg, and P. Abbeel, “Adversarial motion priors make good substitutes for complex reward functions,” in *2022 IEEE/RSJ International Conference on Intelligent Robots and Systems (IROS)*, pp. 25–32, IEEE, 2022. 3
- [37] I. Kato, S. Ohteru, K. Shirai, T. Matsushima, S. Narita, S. Sugano, T. Kobayashi, and E. Fujisawa, “The robot musician ‘wobot-2’(waseda robot-2),” *Robotics*, vol. 3, no. 2, pp. 143–155, 1987. 3
- [38] J.-C. Lin, H.-H. Huang, Y.-F. Li, J.-C. Tai, and L.-W. Liu, “Electronic piano playing robot,” in *2010 International Symposium on Computer, Communication, Control and Automation (3CA)*, vol. 2, pp. 353–356, IEEE, 2010. 3
- [39] T. Maloney, “Piano-playing robotic arm,” tech. rep., 2019. 3
- [40] J. Hughes and P. Maiolino, “An anthropomorphic soft skeleton hand exploiting conditional models for piano playing,” *Science Robotics*, vol. 3, no. 25, 2018. 3
- [41] R. Castro Ornelas, *Robotic Finger Hardware and Controls Design for Dynamic Piano Playing*. PhD thesis, Massachusetts Institute of Technology, 2022. 3
- [42] D. Zhang, J. Lei, B. Li, D. Lau, and C. Cameron, “Design and analysis of a piano playing robot,” in *2009 International Conference on Information and Automation*, pp. 757–761, 2009. 3
- [43] Y.-F. Li and L.-L. Chuang, “Controller design for music playing robot—applied to the anthropomorphic piano robot,” in *2013 IEEE 10th International Conference on Power Electronics and Drive Systems (PEDS)*, pp. 968–973, IEEE, 2013. 3
- [44] A. Zhang, M. Malhotra, and Y. Matsuoka, “Musical piano performance by the act hand,” in *2011 IEEE international conference on robotics and automation*, pp. 3536–3541, IEEE, 2011. 3
- [45] B. Scholz, *Playing Piano with a Shadow Dexterous Hand*. PhD thesis, Universität Hamburg, 2019. 3
- [46] “Shadow Dexterous Hand,” 2005. 3, 4
- [47] S. Yeon, “Playing piano with a robotic hand,” 2022. 3
- [48] H. Xu, Y. Luo, S. Wang, T. Darrell, and R. Calandra, “Towards learning to play piano with dexterous hands and touch,” in *2022 IEEE/RSJ International Conference on Intelligent Robots and Systems (IROS)*, pp. 10410–10416, IEEE, 2022. 3
- [49] A. Muldal, Y. Doron, J. Aslanides, T. Harley, T. Ward, and S. Liu, “dm_env: A python interface for reinforcement learning environments,” 2019. 4
- [50] G. Brockman, V. Cheung, L. Pettersson, J. Schneider, J. Schulman, J. Tang, and W. Zaremba, “Openai gym,” 2016. 4
- [51] E. Todorov, T. Erez, and Y. Tassa, “Mujoco: A physics engine for model-based control,” in *2012 IEEE/RSJ International Conference on Intelligent Robots and Systems*, pp. 5026–5033, IEEE, 2012. 4
- [52] S. Tunyasuvunakool, A. Muldal, Y. Doron, S. Liu, S. Bohez, J. Merel, T. Erez, T. Lillicrap, N. Heess, and Y. Tassa, “dm_control: Software and tasks for continuous control,” *Software Impacts*, vol. 6, p. 100022, 2020. 4
- [53] M. M. Contributors, “MuJoCo Menagerie: A collection of high-quality simulation models for MuJoCo,” 2022. 4
- [54] K. M. Instruments, “Kawai Vertical Piano Regulation Manual,” 2019. 4
- [55] E. Nakamura, Y. Saito, and K. Yoshii, “Statistical learning and estimation of piano fingering,” *ArXiv*, vol. abs/1904.10237, 2019. 5
- [56] T. Hiraoka, T. Imagawa, T. Hashimoto, T. Onishi, and Y. Tsuruoka, “Dropout q-functions for doubly efficient reinforcement learning,” *International Conference on Learning Representations (ICLR)*, 2022. 6, 12
- [57] T. Haarnoja, A. Zhou, P. Abbeel, and S. Levine, “Soft actor-critic: Off-policy maximum entropy deep reinforcement learning with a stochastic actor,” in *ICML*, 2018. 6
- [58] J. Schulman, F. Wolski, P. Dhariwal, A. Radford, and O. Klimov, “Proximal policy optimization algorithms,” *ArXiv*, vol. abs/1707.06347, 2017. 6, 13
- [59] A. Raffin, A. Hill, A. Gleave, A. Kanervisto, M. Ernestus, and N. Dormann, “Stable-baselines3: Reliable reinforcement learning implementations,” *Journal of Machine Learning Research*, vol. 22, no. 268, pp. 1–8, 2021. 6
- [60] T. A. Howell, N. Gileadi, S. Tunyasuvunakool, K. Zakkka, T. Erez, and Y. Tassa, “Predictive sampling: Real-time behaviour synthesis with mujoco,” *ArXiv*, vol. abs/2212.00541, 2022. 6, 7, 13
- [61] Y. Tassa, T. Erez, and E. Todorov, “Synthesis and stabi-

lization of complex behaviors through online trajectory optimization,” *2012 IEEE/RSJ International Conference on Intelligent Robots and Systems*, pp. 4906–4913, 2012. 6

- [62] J. Bradbury, R. Frostig, P. Hawkins, M. J. Johnson, C. Leary, D. Maclaurin, G. Necula, A. Paszke, J. VanderPlas, S. Wanderman-Milne, and Q. Zhang, “JAX: composable transformations of Python+NumPy programs,” 2018. 7, 12
- [63] H. van Hasselt, A. Guez, and D. Silver, “Deep reinforcement learning with double q-learning,” *arXiv e-prints*, 2015. 12
- [64] S. Fujimoto, H. van Hoof, and D. Meger, “Addressing function approximation error in actor-critic methods,” in *Proceedings of the 35th International Conference on Machine Learning, ICML 2018, Stockholmsmassan, Stockholm, Sweden, July 10-15, 2018*, 2018. 12
- [65] N. Srivastava, G. E. Hinton, A. Krizhevsky, I. Sutskever, and R. Salakhutdinov, “Dropout: a simple way to prevent neural networks from overfitting,” *J. Mach. Learn. Res.*, vol. 15, pp. 1929–1958, 2014. 12
- [66] J. Ba, J. R. Kiros, and G. E. Hinton, “Layer normalization,” *ArXiv*, vol. abs/1607.06450, 2016. 12
- [67] X. Glorot and Y. Bengio, “Understanding the difficulty of training deep feedforward neural networks,” in *International Conference on Artificial Intelligence and Statistics*, 2010. 12
- [68] D. P. Kingma and J. Ba, “Adam: A method for stochastic optimization,” *CoRR*, vol. abs/1412.6980, 2014. 12

A. Model-free reinforcement learning

Computing infrastructure and experiment running time

Our model-free RL codebase is implemented in JAX [62]. Experiments were performed on a Google Cloud `n1-highmem-64` machine with an Intel Xeon E5-2696V3 Processor hardware with 32 cores (2.3 GHz base clock), 416 GB RAM and 4 Tesla K80 GPUs. Each “run”, i.e., the training and evaluation of a policy on one task with one seed, took an average of 5 hrs wall clock time. These run times are recorded while performing up to 8 runs in parallel.

Network architecture

We use a regularized variant of clipped double Q-learning [63, 64], specifically DroQ [56], for the critic. Each Q-function is parameterized by a 3-layer multi-layer perceptron (MLP) with ReLU activations. Each linear layer is followed by dropout [65] with a rate of 0.01 and layer normalization [66]. The actor is implemented as a `tanh-diagonal-Gaussian`, and is also parameterized by a 3-layer MLP that outputs a mean and covariance. Both actor and critic MLPs have hidden layers with 256 neurons and their weights are initialized with Xavier initialization [67], while their biases are initialized to zero.

Training and evaluation

We first collect 5000 seed observations with a uniform random policy, after which we sample actions using the RL policy. We then perform one gradient update every time we receive a new environment observation. We use the Adam [68] optimizer for neural network optimization. Evaluation happens in parallel in a background thread every 10000 steps. The latest policy checkpoint is rolled out by taking the mean of the output (i.e., no sampling). Since our environment is “fixed”, we perform only one rollout per evaluation.

Reward formulation

The reward function for training the model-free RL baseline consists of four terms: 1) a key press term r_{key} , 2) a move finger to key term r_{finger} , 3) a forearm collision term r_{forearm} and 4) an energy penalty term r_{energy} .

r_{key} encourages the policy to press the keys that need to be pressed and discourages it from pressing keys that shouldn’t be pressed. It is implemented as:

$$r_{\text{key}} = 0.5 \cdot \left(\frac{1}{K} \sum_i^K g(\|k_s^i - 1\|_2) \right) + 0.5 \cdot (1 - \mathbf{1}_{\{\text{false positive}\}}),$$

where K is the number of keys that need to be pressed at the current timestep, k_s is the normalized joint position of the key between 0 and 1, and $\mathbf{1}_{\{\text{false positive}\}}$ is an indicator function that is 1 if any key that should not be pressed creates a sound (i.e., its normalized joint position crossed 0.5). g is the tolerance function from the `dm_control` [32] library: it takes the L2 distance of k_s and 1 and converts it into a bounded positive number between 0 and 1. We use the parameters `bounds=0.05` and `margin=0.5`.

r_{finger} encourages the fingers that are active at the current timestep to move as close as possible to the keys they need to

press. It is implemented as:

$$r_{\text{finger}} = \frac{1}{K} \sum_i^K g(\|p_f^i - p_k^i\|_2),$$

where p_f is the Cartesian position of the finger and p_k is the Cartesian position of a point centered at the surface of the key. g for this reward is parameterized by `bounds=0.01` and `margin=0.1`.

r_{forearm} encourages the shadow hand forearms not to collide. It is implemented as:

$$r_{\text{forearm}} = 1 - \mathbf{1}_{\{\text{collision}\}},$$

where $\mathbf{1}_{\{\text{collision}\}}$ is 1 if the forearms are in collision and 0 otherwise.

Finally, r_{energy} penalizes high energy expenditure and is implemented as:

$$r_{\text{energy}} = |\tau_{\text{joints}}|^T |v_{\text{joints}}|,$$

where τ_{joints} is a vector of joint torques and v_{joints} is a vector of joint velocities.

The final reward function sums up the aforementioned terms as follows:

$$r_{\text{total}} = r_{\text{key}} + r_{\text{finger}} + 0.4 \cdot r_{\text{forearm}} - 0.005 \cdot r_{\text{energy}}$$

Other hyperparameters

For a comprehensive list of hyperparameters used for training the model-free RL policy, see Table IV.

Hyperparameter	Value
Total train steps	1M
Optimizer	
Type	ADAM
Learning rate	3×10^{-4}
β_1	0.9
β_2	0.999
Critic	
Hidden units	256
Hidden layers	3
Non-linearity	ReLU
Dropout rate	0.01
Actor	
Hidden units	256
Hidden layers	3
Non-linearity	ReLU
Misc.	
Discount factor	0.99
Minibatch size	256
Replay period every	1 step
Eval period every	10000 step
Number of eval episodes	1
Replay buffer capacity	1M
Seed steps	5000
Critic target update frequency	1
Actor update frequency	1
Critic target EMA momentum (τ_Q)	0.005
Actor log std dev. bounds	$[-20, 2]$
Entropy temperature	1.0
Learnable temperature	True

TABLE IV: Hyperparameters for all model-free RL experiments.

B. Model predictive control

Computing infrastructure and experiment running time

Our model-based codebase is implemented in C++ with MJPC [60]. Experiments were performed on a 2021 M1 Max Macbook Pro with 64 GB of RAM.

Algorithm

We use MPC with Predictive Sampling (PS) as the planner. PS is a derivative-free sampling-based algorithm that iteratively improves a nominal sequence of actions using random search. Concretely, N candidates are created at every iteration by sampling from a Gaussian with the nominal as the mean and a fixed standard deviation σ . The returns from the candidates are evaluated, after which the highest scoring candidate is set as the new nominal. The action sequences are represented with cubic splines to reduce the search space and smooth the trajectory. In our experiments, we used $N = 10$, $\sigma = 0.05$, and a spline dimension of 2. We plan over a horizon of 0.2 seconds, use a planning time step of 0.01 seconds and a physics time step of 0.005 seconds.

Cost formulation

The cost function for the MPC baseline consists of 2 terms: 1) a key press term c_{key} , 2) and a move finger to key term c_{finger} .

The costs are implemented similarly to the model-free baseline, but don't make use of the g function, i.e., they solely consist in unbounded l2 distances.

The total cost is thus:

$$c_{\text{total}} = c_{\text{key}} + c_{\text{finger}}$$

Note that we experimented with a control cost and an energy cost but they decreased performance so we disabled them.

C. ROBOPIANIST-prelude

PPO baseline

As mentioned in Section IV, we experimented with training a model-free policy with PPO [58], but found that it performed much worse than DroQ both in terms of sample efficiency and wall clock time. In Figure 8, we report the results of the full training run on ROBOPIANIST-prelude.

D. ROBOPIANIST-repertoire-150

The per-MIDI performance of the MPC baseline is illustrated in Figure 9.

E. ROBOPIANIST-etude-12

As mentioned in Section V, we consider a smaller subset of the full repertoire (12 randomly sampled MIDI files) and report the performance of the model-free and model-based baselines. These results are summarized in Figure 11 and Table V.

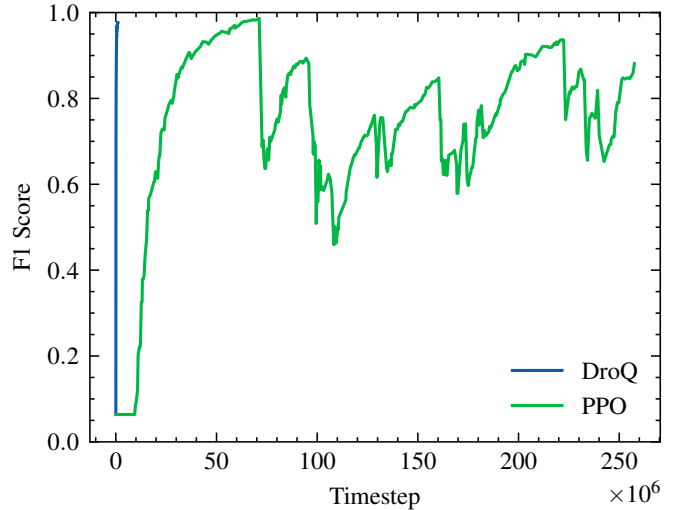


Fig. 8: Performance of DroQ vs PPO on ROBOPIANIST-prelude.

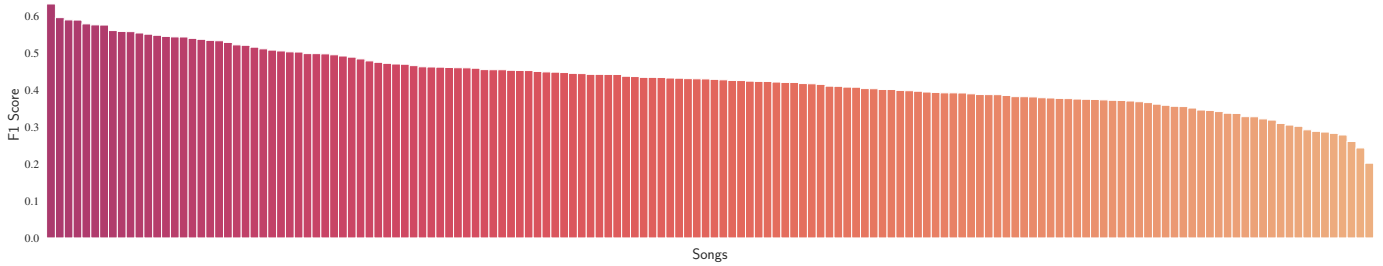


Fig. 9: Full set of F1 scores achieved by the model-based MPC baseline on all tasks in ROBOPIANIST-REPertoire-150.

Baseline	Avg. F1	Avg. Precision	Avg. Recall
Model-free RL	0.538 ± 0.122	0.990 ± 0.006	0.462 ± 0.109
MPC (100% realtime)	0.266 ± 0.079	0.816 ± 0.073	0.225 ± 0.084
MPC (80% realtime)	0.276 ± 0.069	0.813 ± 0.076	0.233 ± 0.081
MPC (20% realtime)	0.402 ± 0.056	0.786 ± 0.060	0.351 ± 0.064
MPC (10% realtime)	0.433 ± 0.072	0.775 ± 0.059	0.385 ± 0.077

TABLE V: **robopianist-etude-12**: Aggregate scores for model-free and model-based baselines averaged over all 12 MIDI files in the etude. The scores for the model-free baseline are obtained from the final checkpoint at 1M steps.

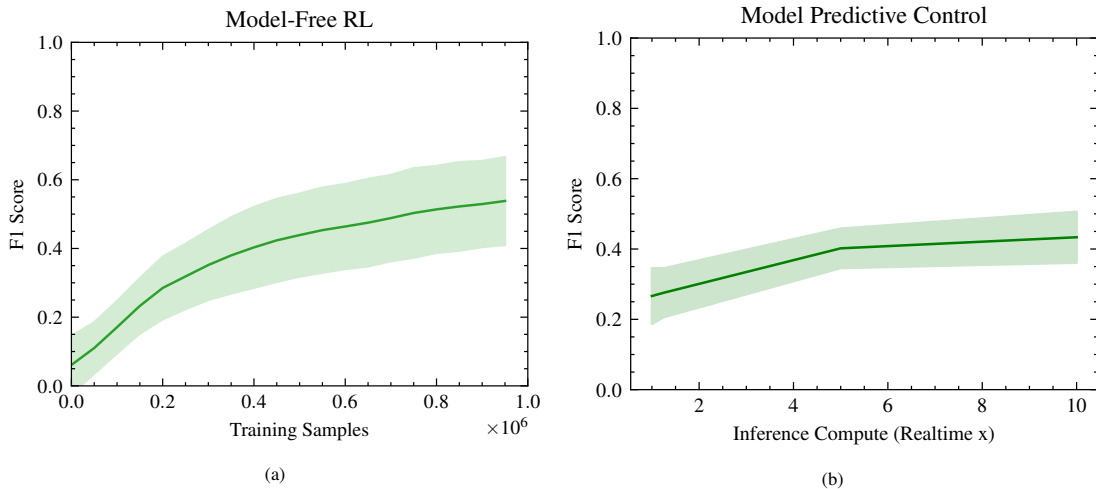


Fig. 11: **ROBOPIANIST-etude-12**: (a) Performance of the model-free RL baseline evaluated at checkpoints trained on increasing amounts of environment interactions. Each point corresponds to an average over 12 MIDI files, 3 seeds each, with a standard deviation shading computed over all MIDI files. (b) Performance of the MPC baseline evaluated with an increasing compute budget (e.g., 2 = double the compute used by the same method running realtime). Each point corresponds to an average over 12 songs, with a standard deviation shading computed over all MIDI files.